

Single-cycle terahertz electromagnetic pulses: A new test bed for physical seismic modeling

Timothy D. Dorney*, Molly J. Rossow[†], William W. Symes*,
and Daniel M. Mittleman[‡]

ABSTRACT

We describe a new technique for physical modeling, based on the use of short pulses of electromagnetic radiation. We employ radiation at a frequency near 1 THz (10^{12} Hz), corresponding to a wavelength of ~ 0.3 mm. Very recent advances in optoelectronic techniques have enabled the generation and detection of broadband terahertz pulses using compact room-temperature transducers. These pulses can be used to form images in a variety of modes, including a multistatic reflection configuration which mimics that of many seismic surveys. We illustrate the capabilities of the modeling technique with a simple experiment which demonstrates accurate surface reconstruction using migration techniques. With respect to conventional modeling techniques using piezoelectric transducers and microphones, the use of terahertz pulses has both benefits and limitations. To our knowledge, this work represents the first use of electromagnetic radiation for modeling acoustic imaging problems.

INTRODUCTION

Physical modeling has been a valuable tool in seismic research for many years (Nelson, 1983). In conjunction with numerical modeling, experiments on physical models can provide valuable insight into the relationships between measured seismic traces and the geologic discontinuities which produced them. In recent years, physical models have been used to explore the effects of subsurface fractures (Ass'ad et al., 1993; Chang and Gardner, 1997; Gibson et al., 2000; Tatham et al., 1992), inhomogeneous or multicomponent media (Ass'ad et al., 1996; Nishizawa et al., 1997; Purnell, 1986), and media with inherent anisotropy (Brown et al., 1991; Varadé

et al., 1996). Careful studies using physical modeling have been useful in clarifying issues such as the detectability and lateral resolution for small targets (Pant and Greenhalgh, 1989b) and the efficacy of saw cuts in blocking surface waves (Pant and Greenhalgh, 1989a). Physical models have also been used extensively in the verification of new theoretical constructs for inversion (Macdonald et al., 1987; Pratt, 1999) and waveform propagation (Chen, 1996). In almost all cases, the physical model is interrogated using acoustic signals generated with piezoelectric transducers.

Here, we describe a new technology for physical modeling which relies on the use of transient electromagnetic impulses, rather than acoustic impulses, for the study of model systems. This method is based on terahertz (THz) time-domain spectroscopy (THz-TDS), a relatively new optoelectronic technique for the generation and detection of few-cycle pulses of far infrared radiation (Smith et al., 1988; van Exter and Grischkowsky, 1990). The central frequency of this optical radiation is in the vicinity of 1 THz (10^{12} Hz), corresponding to a free-space wavelength of ~ 0.3 mm. Submillimeter-wave radiation is the shortest wavelength for which the electric field $E(t)$ [as opposed to the intensity $I(t) \propto |E(t)|^2$] can easily be measured directly. As a result, scale model measurements using THz-TDS are relatively simple and quite compact, easily fitting on a tabletop. Cheville and Grischkowsky (1995) used THz-TDS in studies of bistatic impulse ranging, in which ultra-wideband radar targets were scaled in size by a factor of 200. With recent advances in the capabilities of this novel technology, one can now configure a THz-TDS system in experimental arrangements which mimic those of seismic tomography. We have recently reported the first THz images formed using Kirchhoff migration methods (Dorney et al., 2001). This opens up new possibilities for physical modeling with electromagnetic radiation.

Using THz-TDS for such measurements provides a unique new set of capabilities and advantages. As with all physical

Manuscript received by the Editor December 26, 2001; revised manuscript received June 4, 2002.

*Formerly Rice University, Department of Electrical and Computer Engineering, MS 366, Houston, Texas 77251-1892; presently Rosenthal & Osha L.L.P., One Houston Center, Suite 2800, 1221 McKinney Street, Houston, Texas 77010. E-mail: dorney@rossha.com.

[†]Rice University, Department of Electrical and Computer Engineering, MS 366, Houston, Texas 77251-1892. E-mail: mrossow@rice.edu; daniel@rice.edu.

[‡]Rice University, Department of Computational and Applied Mathematics, MS 134, Houston, Texas 77251-1892. E-mail: symes@rice.edu.

© 2003 Society of Exploration Geophysicists. All rights reserved.

models, it is obviously much less costly to perform laboratory experiments than field seismic measurements. Synthetic models can be constructed with essentially arbitrary precision, so accurate comparisons can be made with the images formed using the acquired data. In addition, there are several important distinctions between electromagnetic and acoustic waves which could be exploited in such measurements. The free-space THz radiation emerges from the emitter as an approximate spherical wave, but the wavefront can easily be collimated or manipulated using lenses or other bulk optical components. As a result, one can form many different wave fronts, ranging from narrow, low-divergence beams to nearly ideal spherical waves. Unlike seismic waves, electromagnetic waves are always polarized in a direction orthogonal to the propagation direction, so there is no analog of P waves or of such phenomena as PSSP mode-conversion (Tatham et al., 1983). However, arbitrary combinations of the two existing transverse polarizations can be generated, and birefringent effects are readily observed. A wide range of transparent materials are available with tabulated wave velocities for use in constructing model samples with known properties. Finally, the use of electromagnetic radiation eliminates the issue commonly encountered in the use of piezoelectric transducers, involving the strong sensitivity to the contact conditions caused by the strong impedance mismatch between the transducer and the surrounding medium.

In this paper, we explore the possibility of configuring THz-TDS in direct analogy to seismic surveys, and thus demonstrate its value as a new alternative for physical modeling. In the first section of this paper, we describe the operations of the THz system used for these measurements. We then describe a measurement to image a complex reflecting surface, which serves to demonstrate the viability of the system for modeling.

TERAHERTZ TIME-DOMAIN SPECTROSCOPY

Until the late 1980s, the ability to readily explore the electromagnetic spectrum in the far infrared or THz region was limited, due to the low intensity or cumbersome nature of THz sources and the poor sensitivity of bolometric (thermal) detectors. This has led to the oft-used term “terahertz gap” to describe the difficult region lying at frequencies too high for conventional electronics, but too low for most optical techniques. Within the last decade, however, there has been a renaissance in the THz field, as several revolutionary new methods for generation and detection have been developed. One of the most mature of these is THz-TDS, in which the THz electric field $E_{THz}(t)$ is measured directly using a coherent sampling technique.

The THz-TDS system relies on lasers which generate optical pulses of ~ 100 fs duration ($1 \text{ fs} = 10^{-15} \text{ s}$). Such lasers are by now standard laboratory tools; reliable turnkey systems are available commercially. To generate THz radiation, a train of ultrafast optical pulses is focused onto a specially designed antenna (Smith et al., 1988; van Exter and Grischkowsky, 1990). A schematic of this transmitter setup is shown in Figure 1. The antenna consists of a simple metal pattern lithographically deposited on a semiconducting substrate, typically gallium arsenide (GaAs). If the laser beam is not present, then under the influence of a dc bias ($\sim 20 \text{ V}$), no current flows across the antenna gap because the semiconductor is insulating at room temperature. However, when a short optical pulse is

absorbed by the GaAs, electrons are promoted to the conduction band of the substrate, and the region in which the laser is focused becomes conducting. This gives rise to a transient current $J(t)$ flowing across the gap, which acts as a radiating dipole and generates a short burst of THz radiation according to $E(t) \propto \partial J(t)/\partial t$. Because of the properties of a dipole at the interface between air and a high dielectric, most of the radiation is emitted into the substrate (Jepsen and Keiding, 1995). A hemispherical lens is attached to the back of the substrate, in order to efficiently couple the radiation into free space (Fattinger and Grischkowsky, 1989). A train of THz pulses is generated, one for each femtosecond optical pulse reaching the detector, at a rate of typically 100 MHz. Subsequently, free-space optics (e.g., lenses, mirrors) can be used to collimate, focus, or otherwise transport the THz beam. With the exception of water vapor (van Exter et al., 1989), air is essentially transparent to THz radiation, so the beam can propagate several meters without significant distortion.

The detection scheme uses a device which is quite similar to the transmitter shown in Figure 1. Here, the antenna is not biased, but instead an ammeter is connected across the terminals. The incoming THz pulse train is focused by the substrate lens onto the antenna gap. The polarized THz pulses act as a transient voltage across the terminals and can drive a current when there are electrons present in the conduction band of the semiconducting substrate. As in the case of the transmitter, a femtosecond optical pulse is used to convert the insulating substrate into a conductor through optical absorption. However, in the case of the receiver, the material is engineered such that the electrons generated in the conduction band by the optical pulse recombine or trap very rapidly. As a result, this detector

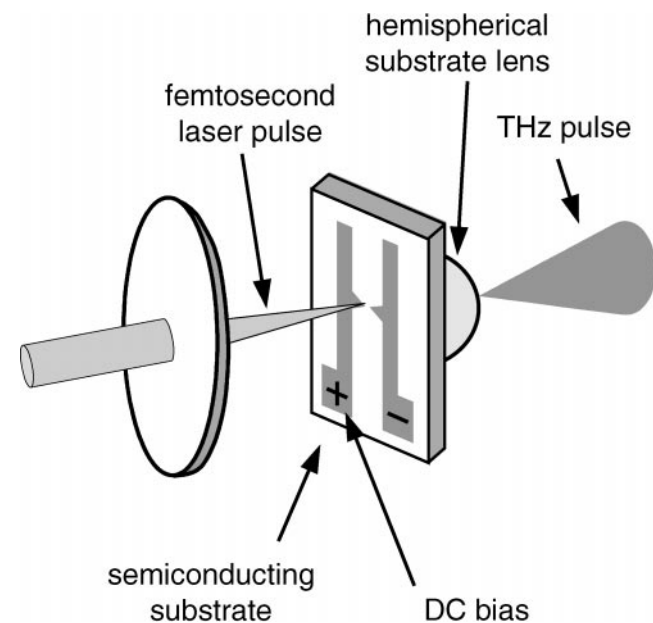


FIG. 1. Schematic of an Auston switch, used to generate single-cycle bursts of THz radiation. A subpicosecond optical pulse excites the semiconducting substrate in a region between two biased electrodes. A rapid change in the current flow across this gap acts as a radiating dipole, sending most of its energy into the high-dielectric substrate. This radiation is coupled into free space using a hemispherical substrate lens.

is sensitive to the incoming THz field for only a very short window of time, during and shortly after the arrival of the optical pulse. This can then be used as a sampling gate to measure the THz field. The arrival time of the optical gating pulse train is synchronized with the arrival time of the THz pulse train, and the delay between the two is slowly swept using an optical delay generator (Smith et al., 1988; Hu and Nuss, 1995). At each delay, the THz waveform is sampled by measuring the current induced in the receiver antenna. The result is a measurement of the photocurrent as a function of the delay, which is essentially proportional to the electric field of the THz radiation. This method of photoconductive sampling has been shown to be sensitive to frequencies as high as 5 THz (Ralph et al., 1994).

A typical measured THz waveform and the corresponding spectrum (obtained by Fourier transform) are shown in Figure 2. The waveform is approximately a single cycle of the electromagnetic field, and the corresponding spectrum is quite broad, spanning more than 1 THz of useful bandwidth. This

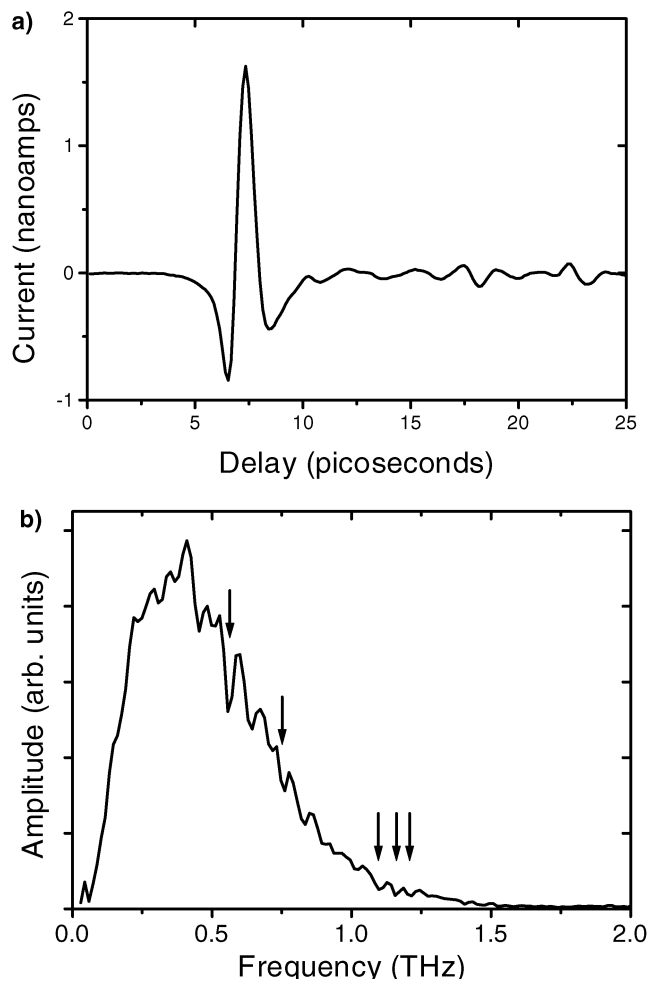


FIG. 2. (a) A typical waveform, measured using the technique described in the text. The signal is essentially proportional to the THz electric field $E_{THz}(t)$, which consists of approximately one optical cycle. (b) The amplitude spectrum $|E(\nu)|$ of the waveform in (a), obtained by Fourier transform. This broadband spectrum ranges from ~ 100 GHz to more than 1.5 THz. The arrows indicate the locations of narrow absorption lines arising from water vapor in the beam path.

detection scheme is unique among THz technologies, since the components operate at room temperature. Normally, in order to sense THz radiation, one needs to use cryogenics to cool the detector so that it is not swamped by thermal radiation. However, in THz-TDS, the gated detection, combined with the fact that only coherent (i.e., not randomly polarized) radiation can generate a nonzero photocurrent, serves to reject thermal radiation to an extraordinary degree. This method provides a sensitivity which exceeds that of the most sophisticated thermal detectors, despite operating at room temperature (van Exter and Grischkowsky, 1990). As a result, the THz field can be measured with a signal-to-noise ratio exceeding 10^4 , even though the intensity of the generated radiation is about 100 times less than that of a room temperature thermal source. The generated radiation is nearly linearly polarized, with a small orthogonally polarized component due to the quadrupole moment of the emitting antenna (Rudd et al., 2000a, 2001). Polarizing filters are readily available and can be used to generate a purer polarization if required.

In 1995, the first imaging system based on THz-TDS was introduced (Hu and Nuss, 1995). This system acquired up to 20 THz waveforms per second, simply by rapidly sweeping the optical delay and using a high-speed analog-to-digital converter for data acquisition. The “T-ray” images in that work, and others that followed, demonstrated a broad range of applications. Subsequently, a number of new imaging modalities have been described in which the unique properties of the THz pulses have been exploited (Mittleman et al., 1997; Johnson et al., 2001; O’Hara and Grischkowsky, 2001). These demonstrations have sparked a great deal of interest because there appear to be many possible commercial applications of “T-ray” imaging. As a result, in February 2000, the first commercial THz system was introduced (Rudd et al., 2000b). In this system, the optical pulses are delivered to both the transmitter and receiver antennas via optical fiber. This affords a tremendous advantage, since, for the first time, multistatic imaging is now possible using THz-TDS (Dorney et al., 2001; Ruffin et al., 2001). Although the system has only one transmitter and one receiver, it is possible to simulate the presence of multiple receivers by repositioning the receiver at many different locations. Because of the fiber coupling, this repositioning does not change the alignment of the optical beam onto the antenna, which would completely alter both the sensitivity and the delay calibration. The receiver antenna exhibits some angular sensitivity (Jepsen and Keiding, 1995; Rudd et al., 2001), but this can be compensated by rotating the receiver as it is repositioned such that it always faces the target, as shown in Figure 3.

EXPERIMENTAL ARRANGEMENT AND RESULTS

To demonstrate the utility of the THz system as a test bed, we acquire waveforms in a method that mimics the approach for marine multichannel reflection surveys (Dobrin and Savit, 1988). We translate the receiver along a line, and rotate it to compensate for its angular sensitivity. Great care is taken to ensure that this rotation is about an axis through the receiver antenna, so that it does not alter the traveltime of the pulse reflected from the target. The configuration shown in Figure 3 mimics the geometry of a typical two-dimensional seismic survey, where the transmitter is a device for generating a seismic impulse (e.g., dynamite or air gun) and the receivers are an

array of geophones or hydrophones. The transmitter, receiver, and target can be automatically repositioned and reoriented using motorized stages. In this demonstration experiment, only a two-dimensional image is acquired; the target is translationally invariant along the direction orthogonal to the plane of the page in Figure 3.

In this model experiment, the target is a metal reflector, bent so that it mimics the anticlines and synclines of a buried interface. The perpendicular distance from the transmitter and receiver to the target is approximately 135 mm. For these measurements, the central frequency of the THz pulse is about 0.4 THz (see Figure 2), corresponding to a wavelength of 0.75 mm in free space. Thus, the reflector is situated approximately 180 wavelengths from the transmitter. This scaling is comparable to typical situations in seismic studies, in which features at several kilometers depth are imaged using acoustic wavelengths of tens to hundreds of meters. The THz system offers a great deal of flexibility with regard to the relative locations and orientations of the sample, the transmitter, and the receiver.

For each fixed transmitter-to-receiver offset, we translated the target to 90 different positions, in 1-mm steps, and acquired a complete THz waveform at each target position. The transmitter-to-receiver offset was adjusted in 1-mm increments after each complete target translation. The transmitter-to-receiver offset ranged from approximately 30 to 150 mm. Because of the size of the housings containing the two antennas, an offset smaller than 30 mm was not possible in these measurements. The complete data set is representative of a towed streamer array with a single source and 121 towed receivers moving over a section of the target. Figure 4 shows

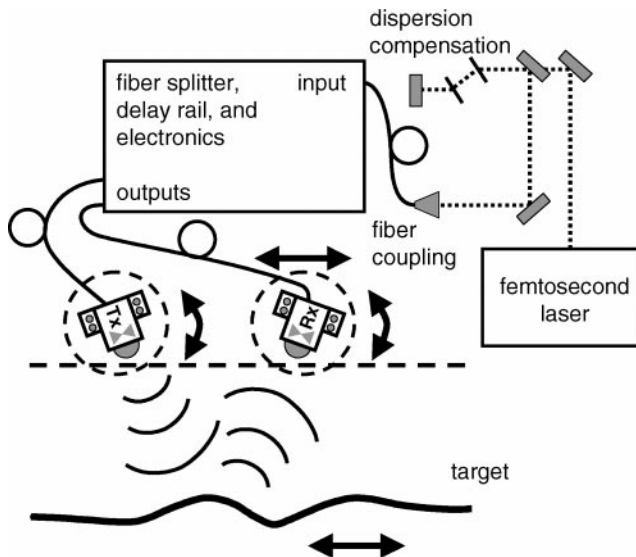


FIG. 3. Schematic of the fiber-coupled THz system used for these measurements. This system provides a constant temporal delay as the transmitter and receiver are translated because of the fixed length of the fiber optic cable used to deliver the femtosecond pulses to the antennas. To simulate simultaneous multistatic data acquisition, we translate the receiver along a line. The receiver is rotated as it is translated in order to compensate for its angular sensitivity. The target is a metal plate (reflector) bent to create two anticlines and one included syncline, as shown.

common offset data from the bent reflecting target with the transmitter-to-receiver offset at 34 mm. We note the expected butterfly reflections from the two anticline and included syncline surface. This mimics the simulated experiment presented by Scales (1995).

In most seismic acquisition systems, the absolute propagation time is known (since $t=0$ is set by the detonation of an impulse source) while the wave velocity of the acoustic impulse in the first layer, v_0 , is generally not known. In contrast, in the THz experiment, the wave velocity of the first layer (V_{air}) is known precisely since this layer is simply air, but the time between the emission and detection of the THz pulse is not known since THz-TDS only provides relative delays. In both cases, however, the unknown quantity can be obtained from Green's equation (Green, 1938; Dix, 1955). We collect data using a flat reflector and adjust the time base of all waveforms equally until a plot of T_x^2 versus x^2 produces a straight line with a slope equal to $1/V_{air}^2$. Here, x is the receiver offset and T_x is the absolute transmitter-to-target-to-receiver traveltime for a receiver at offset x . Figure 5 shows the arrival time of the primary reflection from common shot data after the appropriate time shift of the waveforms. The intercept of this line determines the perpendicular distance from the transmitter to the target, and permits us to determine the absolute calibration for the z (depth) axis in Figure 6b.

An important advantage of physical modeling over field geophysical acquisition is the ability to accurately measure the actual target. Borehole and downhole surveys are expensive and obviously not complete. We use a micrometer mounted on a translation stage to profile the reflecting surface, with a step size of 0.5 mm and a resolution of 25 μm . This measurement is shown in Figure 6a. This represents the actual shape of the target surface and can be compared to images formed using the acquired THz data.

We generate an image of the target by computing diffraction sums using all 10 890 acquired THz waveforms, with a migration pixel size of 50 μm . The result is displayed in Figure 6b. This pixel size is more than adequate, considering the horizontal resolution obtained by calculating the size of the first

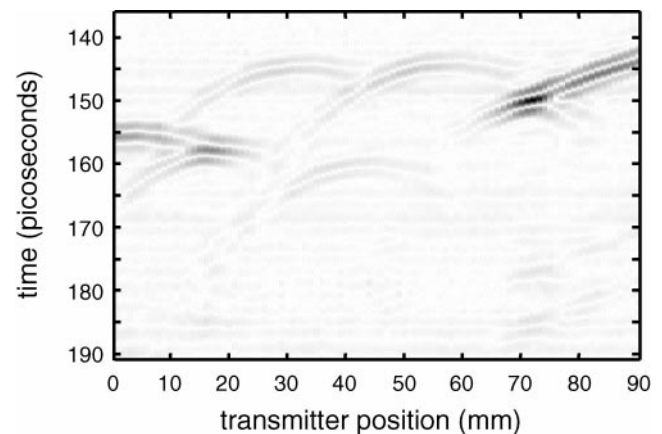


FIG. 4. Common offset data for a 34-mm transmitter-to-receiver offset. The bent reflecting target contains anticlines and a syncline, as shown in Figure 6. The expected butterfly patterns can clearly be observed in the common offset data.

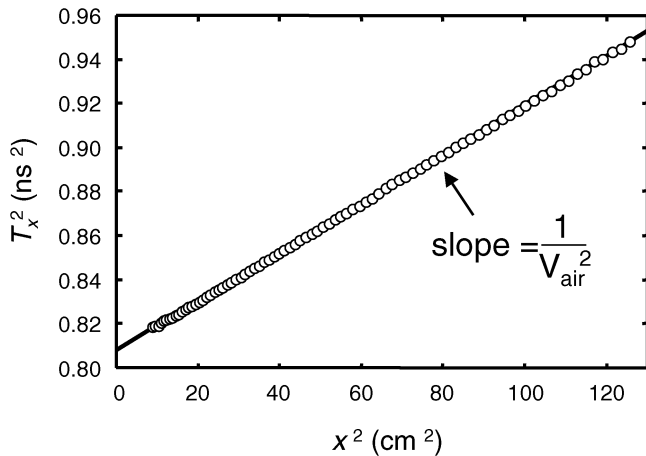


FIG. 5. The absolute propagation time for the THz system is determined by plotting the squared receiver offset for a flat plate, positioned parallel to the transmitter/receiver line. Green's technique (Green, 1938; Dix, 1955) is used to determine the absolute propagation time when the seismic wave velocity V_{air} is known, as described in the text. The squared two-way traveltime is adjusted until the slope equals $1/V_{air}^2$. This procedure is used to calibrate the z (depth) axis in Figure 6b.

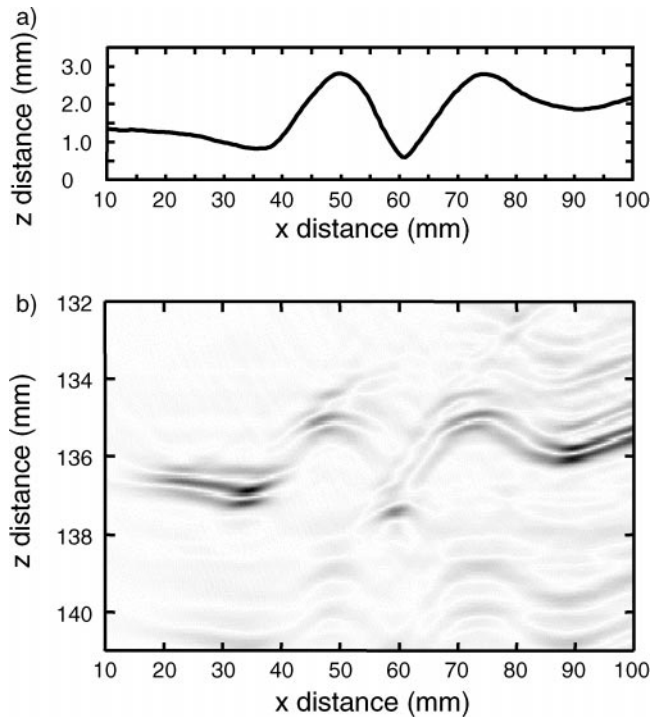


FIG. 6. (a) Micrometer measurements along the plate every 0.5 mm reveal the exact curvature of the surface. (b) Kirchoff (diffraction) summation of the data collected as described in the text. This image was computed using a 50- μ m grid. It clearly shows the two anticlines and included syncline. The vertical scales in (a) and (b) are the same, to facilitate comparisons. The Kirchoff image clearly reproduces the shape of the sample. In this image, the vertical resolution is somewhat less than 1 mm, and could be improved to near the limit imposed by the coherence length of the radiation with appropriate deconvolution of the input pulse shape.

Fresnel zone, $(V_{air}/4)\sqrt{T_{min}/\Delta f} \approx 3.8$ mm (Dobrin and Savit, 1988; Scales, 1995), and the vertical resolution determined from the coherence length, $(V_{air}/\Delta f) \approx 0.21$ mm (Scales, 1995). The axes of this image have been scaled to correspond to those of Figure 6a, to facilitate comparison. As expected, the contours formed in the image correspond almost precisely with the actual shape of the reflecting surface. The blurring of the surface is a result of two factors. The first is a result of the finite pulse-coherence length, which limits the depth resolution. The second, more important factor is that we have not performed any deconvolution procedures to remove the oscillatory shape of the input pulse. Standard techniques for deconvolution and removal of multiples should provide a single edge on the primary reflection and also remove image artifacts such as the echo of the surface at greater depth. Nevertheless, this image clearly demonstrates the homology between the electromagnetic THz system and conventional seismic imaging methods.

DISCUSSION

We demonstrate a new method for physical modeling, based on the use of electromagnetic impulses. The data shown above demonstrate the versatility of terahertz time-domain spectroscopy for modeling of multistatic imaging configurations. This provides an interesting alternative to the more conventional methods of physical modeling using high-frequency acoustic waves. In both cases, the essential idea is to scale the wavelength of the propagating disturbance down to a manageable size, so that the measurement can be performed on a tabletop. If a precise homology with seismic prospecting is desired, it is of course necessary to also scale the properties of the test medium by an equivalent factor, relative to those of the earth. This is an issue in any physical modeling experiment and, in some cases, may dictate the utility of the system. However, it should be noted that inexpensive transparent materials are available with a wide range of properties in the THz spectral range, so interfaces with nearly any desired velocity mismatch can be simulated. For example, high-resistivity silicon has a refractive index which is 3.4 times that of air (Grishkowsky et al., 1990). By doping the silicon, one can add an arbitrary amount of absorption (dissipation of energy) (Jeon and Grishkowsky, 1997). Many plastic materials have indices in the range from 1.4 to 1.8, with varying degrees of transparency (Birch et al., 1981). It is also quite easy to simulate strongly inhomogeneous materials, in which wave propagation may be too complex for numerical modeling (Nishizawa et al., 1997). We have recently described the first measurements of single-cycle optical pulse propagation in a strongly scattering medium (Pearce and Mittleman, 2001). A model sample was constructed using a randomly packed arrangement of polymer spheres of diameter comparable to the wavelength of the radiation. Similar concepts could be used to simulate the properties of inhomogeneous geophysical strata.

This work also offers new possibilities for the evaluation of novel seismic processing algorithms. Generally, such advances in signal processing techniques are evaluated using simulated data for which the effects of scattering or noise can be difficult to emulate. Another option in the testing of new imaging algorithms is to use real data from field studies. In such cases, however, the "correct" answer is usually not known with high precision, so comparisons are not always revealing. A third

option is the use of scale models as test beds, an approach that can provide a valuable new perspective. With the THz system, it is quite simple to fabricate models which emulate challenging situations, such as for example the lensing effects of salt domes. In this situation, it may not be necessary to accurately reproduce scaled replicas of a particular realistic velocity field. Simply reproducing the geometry may be sufficient to provide a test bed with which real-world data can be acquired and new inversion algorithms can be validated or debugged. In this case, the modeling system can provide a useful new perspective, even in the case where the limited range of material properties prohibits the construction of an accurate scale model of the earth.

As a final point, we note that the THz imaging system shares many of the advantages of the more conventional acoustic modeling methods. Because the wavelength is in the submillimeter range, the entire experiment fits on a single table. With the exception of the femtosecond laser, no sophisticated high-speed electronics or equipment are required. Indeed, the cost of the commercial version of the THz imaging system is comparable to the cost of assembling a state-of-the-art acoustic modeling facility. This technique should therefore prove to be a valuable new tool for the seismic imaging community.

ACKNOWLEDGMENTS

We acknowledge partial support for this work by the Environmental Protection Agency and the National Science Foundation. The assistance of J. Van Rudd and Matt Warmuth at Picometrix, Inc. is gratefully acknowledged.

REFERENCES

- Ass'ad, J. M., McDonald, J. A., Tatham, R. H., and Kusky, T. M., 1996, Elastic wave propagation in a medium containing oriented inclusions with a changing aspect ratio: A physical model study: *Geophys. J. Internat.*, **125**, 163–172.
- Ass'ad, J. M., Tatham, R. H., McDonald, J. A., Kusky, T. M., and Jech, J., 1993, A physical model study of scattering of waves by aligned cracks: Comparison between experiment and theory: *Geophys. Prosp.*, **41**, 323–339.
- Birch, J. R., Dromey, J. D., and Lesurf, J., 1981, The optical constants of some common low-loss polymers between 4 and 40 cm^{-1} : *Infr. Phys.*, **21**, 225–228.
- Brown, R. J., Lawton, D. C., and Cheadle, S. P., 1991, Scaled physical modelling of anisotropic wave propagation: Multioffset profiles over an orthorhombic medium: *Geophys. J. Internat.*, **107**, 693–702.
- Chang, C.-H., and Gardner, G. H. F., 1997, Effects of vertically aligned subsurface fractures on seismic reflections: A physical model study: *Geophys.*, **62**, 245–252.
- Chen, G., 1996, Comparison of 2-D numerical viscoelastic waveform modeling with ultrasonic physical modeling: *Geophys.*, **61**, 862–871.
- Chevillat, R. A., and Grischkowsky, D., 1995, Time domain terahertz impulse ranging studies: *Appl. Phys. Lett.*, **67**, 1960–1962.
- Dix, C. H., 1955, Seismic velocities from surface measurements: *Geophys.*, **20**, 68–86.
- Dobrin, M., and Savit, C., 1988, *Introduction to geophysical prospecting*: McGraw-Hill.
- Dorney, T. D., Johnson, J. L., Rudd, J. V., Baraniuk, R. G., Symes, W. W., and Mittleman, D. M., 2001, Terahertz reflection imaging using Kirchhoff migration: *Opt. Lett.*, **26**, 1513–1515.
- Fattinger, C., and Grischkowsky, D., 1989, Terahertz beams: *Appl. Phys. Lett.*, **54**, 490–492.
- Gibson, R. L., Theophanis, S., and Toksöz, M. N., 2000, Physical and numerical modeling of tuning and diffraction in azimuthally anisotropic media: *Geophys.*, **65**, 1613–1621.
- Green, C. H., 1938, Velocity determinations by means of reflection profiles: *Geophys.*, **3**, 295–305.
- Grishkowsky, D., Keiding, S., van Exter, M., and Fattinger, C., 1990, Far-infrared time-domain spectroscopy with terahertz beams of dielectrics and semiconductors: *J. Opt. Soc. Am. B*, **7**, 2006–2015.
- Hu, B. B., and Nuss, M. C., 1995, Imaging with terahertz waves: *Opt. Lett.*, **20**, 1716–1719.
- Jeon, T.-I., and Grischkowsky, D., 1997, Nature of conduction in doped silicon: *Phys. Rev. Lett.*, **78**, 1106–1109.
- Jepsen, P., and Keiding, S. R., 1995, Radiation patterns from lens-coupled terahertz antennas: *Opt. Lett.*, **20**, 807–809.
- Johnson, J. L., Dorney, T. D., and Mittleman, D. M., 2001, Enhanced depth resolution in terahertz imaging using phase-shift interferometry: *Appl. Phys. Lett.*, **78**, 835–837.
- Macdonald, C., Davis, P. M., and Jackson, D. D., 1987, Inversion of reflection traveltimes and amplitudes: *Geophys.*, **52**, 606–617.
- Mittleman, D. M., Hunsche, S., Boivin, L., and Nuss, M. C., 1997, T-ray tomography: *Opt. Lett.*, **22**, 904–906.
- Nelson, H. R., 1983, New technologies in exploration geophysics: *Gulf Publ. Co.*
- Nishizawa, O., Satoh, T., Lei, X., and Kuwahara, Y., 1997, Laboratory studies of seismic wave propagation in inhomogeneous media using a laser Doppler vibrometer: *Bull. Seism. Soc. Am.*, **87**, 809–823.
- O'Hara, J., and Grischkowsky, D., 2001, Quasi-optic terahertz imaging: *Opt. Lett.*, **26**, 1918–1920.
- Pant, D. R., and Greenhalgh, S. A., 1989a, Blocking surface waves by a cut: Physical seismic model results: *Geophys. Prosp.*, **37**, 589–605.
- 1989b, Lateral resolution in seismic reflection—A physical model study: *Geophys. J.*, **97**, p. 187–198.
- Pearce, J., and Mittleman, D., 2001, Propagation of single-cycle terahertz pulses in random media: *Opt. Lett.*, **26**, 2002–2004.
- Pratt, R. G., 1999, Seismic waveform inversion in the frequency domain, part 1: Theory and verification in a physical scale model: *Geophys.*, **64**, 888–901.
- Purnell, G. W., 1986, Observations of wave velocity and attenuation in two-phase media: *Geophys.*, **51**, 2193–2199.
- Ralph, S. E., Perkowitz, S., Katzenellenbogen, N., and Grischkowsky, D., 1994, Terahertz spectroscopy of optically thick multilayered semiconductor structures: *J. Opt. Soc. Am. B*, **11**, 2528–2532.
- Rudd, J. V., Johnson, J. L., and Mittleman, D. M., 2000a, Quadrupole radiation from terahertz dipoles: *Opt. Lett.*, **25**, 1556–1558.
- 2001, Cross-polarized angular emission patterns from lens-coupled terahertz antennas: *J. Opt. Soc. Am. B*, **18**, 1524–1533.
- Rudd, J. V., Zimdars, D., and Warmuth, M., 2000b, Compact fiber-pigtailed terahertz imaging system: *Proc. SPIE*, **3934**, 27–35.
- Ruffin, A. B., Decker, J., Sanchez-Palencia, L., Le Hors, L., Whitaker, J. F., Norris, T. B., and Rudd, J. V., 2001, Time reversal and object reconstruction with single-cycle pulses: *Opt. Lett.*, **26**, 681–683.
- Scales, J., 1995, *Theory of seismic imaging*: Springer-Verlag.
- Smith, P. R., Auston, D. H., and Nuss, M. C., 1988, Subpicosecond photoconducting dipole antennas: *IEEE J. Quant. Elec.*, **24**, 255–260.
- Tatham, R. H., Goolsbee, D. V., Massell, W. F., and Nelson, H. R., 1983, Seismic shear-wave observations in a physical model experiment: *Geophys.*, **48**, 688–701.
- Tatham, R. H., Matthews, M. D., Sekharan, K. K., Wade, C. J., and Liro, L. M., 1992, A physical model study of shear-wave splitting and fracture intensity: *Geophys.*, **57**, 647–652.
- van Exter, M., Fattinger, C., and Grischkowsky, D., 1989, Terahertz time-domain spectroscopy of water vapor: *Opt. Lett.*, **14**, 1128–1130.
- van Exter, M., and Grischkowsky, D., 1990, Characterization of an optoelectronic terahertz beam system: *IEEE Trans. Microwave Th. Tech.*, **38**, 1684–1691.
- Varadé, A., Bayón, A., Rasolofosaon, P. N. J., and Gascón, F., 1996, Experimental results on bulk waves and Rayleigh waves in slate: *J. Acoust. Soc. Am.*, **99**, 292–298.